ROYAL SOCIETY OF CHEMISTRY

PAPER
Alessandra Azzali, José M. Delgado-López *et al.*
A novel engineered nanoherbicide: improving performance, efficiency and sustainability of herbicide bentazon

PAPER

Check for updates

A novel engineered nanoherbicide: improving performance, efficiency and sustainability of herbicide bentazon†

Alessandra Azzali, [ID] ‡*[ab] Cristina Miguel-Rojas, [ID] ‡[c] María C. Alcántara-Braña,[d]
Belén Parra-Torrejón, [ID] [a] Gloria B. Ramírez-Rodríguez, [ID] [a] Fabrizia Grepioni, [ID] [b]
Alejandro Pérez-de-Luque [ID] [c] and José M. Delgado-López [ID] *[a]

A new nanoherbicide using bentazon (Btz), a widely used post-emergence herbicide, was developed in the present work, to considerably reduce the required dosages without compromising its efficacy. Biocompatible and biodegradable nanoparticles (*i.e.* amorphous calcium phosphate, ACP) have been engineered to act as a carrier for the sustained delivery of the herbicide. The resulting nanocomposite (Btz-ACP) was characterized through complementary techniques, such as PXRD, FTIR, TEM, and elemental analysis, confirming the successful loading of Btz onto ACP nanoparticles and the subsequent pH-responsive release of the herbicide in aqueous media. Release kinetic constants of $0.11~h^{-1}$ and $0.2~h^{-1}$ were found at pH 7 and pH 4.5, respectively. We also found that the retention of Btz-ACP was increased in inert soils in comparison to the free herbicide, indicating its potential to mitigate groundwater contamination. This new nanoherbicide allows a significant reduction of herbicide dosage by up to 60% compared to the commercial product at the recommended dosage ($1~kg~ha^{-1}$) to efficiently control the growth of *Sinapis alba* (white mustard). Notably, the most diluted Btz-ACP formulation ($0.4~kg~ha^{-1}$) exhibited the highest weed control at 10 days post treatment ($96.3 \pm 8.8\%$ mortality), outperforming all other tested treatments: commercial formulations ($77.4 \pm 24.5\%$ of mortality at the recommended dose and $74.5 \pm 20.1\%$ at the reduced dose of $0.7~kg~ha^{-1}$) but also higher doses of Btz-ACP ($0.6~kg~ha^{-1}$) ($78.1 \pm 18.9\%$ of mortality) with an inverse concentration–efficiency relationship. This may be due to the reduction of nanoparticle aggregation at low dosages, thus favoring nanoparticle penetration through the leaves. Interestingly, despite the huge reduction of dosage, the herbicidal effect is still visible after 28 days post-treatment, avoiding the regrowth of the target plant. The results demonstrate that this new nanomaterial offers a very promising approach to sustainable agriculture with reduced environmental impact.

Environmental significance

In this work, biocompatible and eco-friendly ACP nanocarriers (which mimic the inorganic fraction of bone) have been used for the reformulation of bentazon, a widely used herbicide, highly leachable and groundwater contaminant. A significant reduction in the required herbicide dosage—up to 60%—can be achieved, while maintaining and even enhancing efficacy. Moreover, the slower release kinetics of the nanoherbicide, combined with prolonged soil retention, suggest potential for decreased contamination risks. Furthermore, the nanocarrier used in this work offers notable advantages, including biocompatibility and biocompatible residues, adherence to green chemistry principles, and scalability. These important advancements pave the way for further research into safer and more effective herbicide formulations and address critical environmental concerns, including inefficient excessive agrochemical use and derived contamination.

[a] *Departamento de Química Inorgánica, Facultad de Ciencias, Universidad de Granada, 18071 Granada, Spain. E-mail: a.azzali@ugr.es, jmdl@ugr.es*
[b] *Dipartimento di Chimica "Giacomo Ciamician", Università di Bologna, Via F. Selmi, 2, 40126 Bologna, Italy*
[c] *Instituto de Investigación y Formación Agraria y Pesquera, Junta de Andalucía, Área de Mejora Vegetal y Biotecnología, Centro Alameda del Obispo, Apdo. 3092, 14080 Córdoba, Spain*

[d] *Instituto de Investigación y Formación Agraria y Pesquera, Junta de Andalucía, Área de Producción Agraria y Protección de Cultivos, Centro Alameda del Obispo, Apdo. 3092, 14080 Córdoba, Spain*
† Electronic supplementary information (ESI) available. See DOI: https://doi.org/10.1039/d5en00195a
‡ Equal contribution to the experimental work of this manuscript.

Introduction

Politics are taking action to regulate the use of agrochemicals due their detrimental environmental impact, as in the case of European Union's Farm to Fork strategy, which seeks to reduce pesticide use by 50% by 2030.[1] Among agrochemicals, herbicides constitute the most extensively employed category, accounting for over 50% of the total pesticide volume sold.[2] Significantly reducing their quantities is imperative to achieve an overall reduction in agrochemical usage. Within the class of herbicides, bentazon, commercially available as Basagran, is a post emergence herbicide that is used to control weeds in various crops like soy (*Glycine max*), peas (*Pisum sativum*), and corn (*Zea mays*). Moreover, bentazon is a selective herbicide that is only effective on broadleaf weeds white mustard (*Sinapis alba*), pigweed (*Amaranthus spp.*), and crabgrass (*Digitaria spp*).[3] It is commercialized as its sodium salt to increase its solubility and ease spray dispersion on the fields. However, it lacks efficiency due to the loss of applied material over the course of its operational lifespan.[4,5] Hence it can be found in groundwater exceeding permitted quantities,[6] due to its high leachability in soil after application.[7,8] Therefore, a new formulation is needed to enhance the efficacy of this herbicide, thereby diminishing the application dosage and subsequently mitigating groundwater and soil contamination. So far, very few studies have been performed in the direction of reformulating this active ingredient to improve its efficacy[5,9–11] and far more were dedicated to the removal of bentazon from wastewaters and soil environments.[12–16]

The exploration of nanomaterials in agriculture as new technologies has been ongoing since the proposal of novel nanoformulations of pesticides and fertilizers.[17–20] In the past decade, new herbicide formulations have been developed to leverage the unique properties of nanoscale materials.[21,22] Most of these studies mainly focused on the development of nanocapsules of synthetic (*e.g.*, polycaprolactone[23,24]) or natural (*e.g.*, chitosan[25,26]) polymers, some of them allowing the stimuli-responsive delivery of the herbicide but demanding difficult synthetic protocols.[26–28] Several studies have evaluated the efficacy of these nanoformulations under controlled conditions, with some demonstrating significant improvements in performance.[25,26,28–30] However, the field of inorganic carriers for nanoherbicides remains largely unexplored. It is also worth mentioning that most of these studies evaluated the action of the new nanoformulation within a few days post treatment (dpt), without assessing the mortality of the target plant at long dpt.[31–33] These data are indeed very relevant to demonstrate the sustained efficacy of the newly-designed nanoherbicide and evaluate the necessity of repeated applications to efficiently kill the plant.

Finally, concerning environmental safety and sustainability, the use of fully biocompatible and biodegradable nanocarriers is of utmost importance to achieve a two-folded aim, *i.e.*, to increase the efficiency of the treatment (reducing dosages) and to reduce the use of chemicals (including solvents) of concern during the whole life cycle (production, use and end-of-life). This must be considered to produce safe and sustainable by design (SSbD)[34] nanomaterials able to really minimize the negative impact on health and the environment. In this view, the synthesis of calcium phosphate nanoparticles, in the form of nanocrystalline apatite or its amorphous precursor (ACP), mimicking the features of the mineral phase of hard tissues (bone, teeth, *etc.*), is of special interest. In fact, biomimetic calcium phosphate nanoparticles are fully biocompatible and unharmful to health and the environment.[35] Moreover, they could be cost-effectively produced, and the synthesis can be easily scaled up, following the green chemistry principles. Although demonstrating promise in agricultural applications,[36–40] amorphous calcium phosphate nanoparticles have not been proposed as herbicide nanocarriers.

It is also highly remarkable that this nanomaterial leaves behind residual compounds that are recognized plant nutrients, Ca^{2+} and PO_4^{3-}, potentially enriching the soil. Therefore, we propose the development of a new nanoherbicide based on biodegradable and biocompatible nanocarriers (ACP) for a more efficient delivery of the herbicide bentazon (Btz). If their combination with a herbicide active ingredient proves to enhance efficacy against the target plant (*Sinapis alba*), while enabling controlled release and reduced soil mobility, they could represent a valuable advancement in the development of SSbD nanoherbicide carriers, especially for the case of bentazon.

Materials and methods

Materials

Analytical-grade reagents were purchased from Sigma-Aldrich: sodium citrate tribasic dihydrate ($Na_3(C_6H_5O_7)\cdot2H_2O$, ≥99.0% pure), potassium phosphate dibasic anhydrous (K_2HPO_4, ≥99.0% pure), potassium hydroxide (KOH 85% pellet for analysis), calcium chloride dihydrate ($CaCl_2\cdot2H_2O$, ≥99.0% pure), and sodium carbonate (Na_2CO_3, ≥99.5% ACS reagent). Bentazon (98%) was purchased from TCI chemicals. Ultrapure water (0.22 μS, 25 °C, Milli-Q, Millipore) was used to prepare the solutions.

Synthesis of ACP

Amorphous calcium phosphate (ACP) nanoparticles were obtained by a simple batch precipitation method consisting in the mixing of two aqueous solutions (1:1 v/v, 200 mL total) at room temperature: (A) $CaCl_2$ (0.2 M) and Na_3Cit (0.2 M) and (B) K_2HPO_4 (0.12 M) and Na_2CO_3 (0.1 M).[41] Carbonate and citrate ions, in the form of sodium salts, were added with the aim of mimicking the composition of bone nanoparticles (in a so-called biomimetic approach).[42] The precipitates were collected after 5 minutes, and then washed three times with ultrapure water by centrifugation (10

4212 | *Environ. Sci.: Nano*, 2025, **12**, 4211–4221

This journal is © The Royal Society of Chemistry 2025

minutes, 13 500 rpm, 10 °C). Nanoparticles were then stored at 4 °C until use.

Bentazon adsorption

20 mg of ACP were placed in a vial and ultrapure water (550 μL) was added and used to resuspend the nanoparticles, with vortex agitation. Then 90 μL of bentazon solution (0.14 M, 20% v/v DMSO/water) was added to the suspended nanoparticles. The solution was left stirring for 24 h at room temperature, protected from the light. After this period the product was centrifuged at 10 000 rpm for 15 minutes and the liquid part with unreacted Btz was removed. The as-obtained ACP nanoparticles functionalized with Btz (Btz-ACP) were stored at 4 °C. A small amount of sample was freeze-dried (Telstar) for further characterization.

Characterization

Powder X-ray diffraction patterns were collected with a benchtop diffractometer (Bruker D2 PHASER) and Bruker D8 Advance diffractometer (from the Centre for Scientific Instrumentation of the University of Granada, CIC-UGR) using Cu Kα radiation (λ = 1.5406 Å), from 15° to 55° (2θ) with a scan rate of 40 s per step and a step size of 0.02° with an HV generator set at 50 kV and 1 mA. Fourier transform infrared (FTIR) spectra were collected on a Tensor 27 (Bruker, Karlsruhe, Germany) spectrometer, between 400 cm^{-1} and 4000 cm^{-1} at a resolution of 4 cm^{-1}, averaged 25 scans. To this aim, 2 mg of freeze-dried sample was mixed with 200 mg of anhydrous KBr and pressed under 5 tons for 1 minute using a hydraulic press (Specac). Pure KBr pellets were used as a reference.

Transmission electron microscopy (TEM) images were acquired with a LIBRA 120 PLUS instrument (Carl Zeiss SMT, CIC-UGR), operating at 120 kV. A STEM FEI TALOS F200X microscope equipped with 4 Super-X SDDs (Thermo Fisher Scientific Waltham, MA) of CIC-UGR was used to further evaluate the composition of Btz-ACP nanoparticles by high-angle annular dark field-scanning transmission electron microscopy (HAADF-STEM) and energy-dispersive X-ray (EDS) spectroscopy. ACP and Btz-ACP nanoparticles were suspended in ultrapure water with sonication for 15 minutes. A 200 mesh copper grid covered with amorphous carbon films was then dipped in the solution and then left to air dry.

The quantity of Btz on the nanoparticles was calculated by analyzing the N percentage in the sample with an organic elemental analyzer FLASH 2000 Thermo Scientific (CIC-UGR) based on flash dynamic combustion. The error between different EA measurements was always <0.12.

Btz release kinetics in aqueous media and simulated soil media (leaching)

Btz release from Btz-ACP nanoparticles was monitored with an Agilent Cary 60 UV-vis spectrophotometer. Btz in solution was quantified considering the strongest absorption band of the bentazon at λ = 333 nm (calibration curve is presented in Fig. S1†). 30 mg of Btz-ACP was weighed in quartz cuvettes and 3 mL of Tris–HCl buffer at pH 7 was added prior to the beginning of the measurement. The absorbance at 333 nm was measured until reaching a plateau, approximately four days. Three repetitions of each sample were averaged and presented in this work. The release curves were fitted to a first-order release model $a \cdot (1 - e^{-kt}) + c$, k being the release rate constant. The same procedure was followed for pH dependent release experiments. Two solutions with pH adjusted to 4.5 were used, one was ultrapure water adjusted with 5 M hydrochloric acid and one was composed of acetate buffer.

Soil leaching experiments were carried out with a vertical column with inert soil consisting of a mixture of vermiculite and sand 1:3. The soil was initially sifted with a colander with 18 mesh grids. To prepare the column, 13 mg of this soil was added in a column and rinsed with ultrapure water until reaching the soil holding capacity (ca. 2 mL). Then 500 μL of Btz or Btz-ACP solutions (2.2 mg mL^{-1} of Btz in both cases) were prepared and were added dropwise to the soil. The quantity of bentazon added to the soil was kept constant in the two experiments; therefore 1.1 mg of Btz was dissolved in ultrapure water with pH adjusted to 12 with NaOH in order to obtain free Btz as a control and for Btz-ACP 418 mg of gel (1.2 mg of Btz) was resuspended. Later, 2 mg of soil was added to top up the column and wetted with 200 μL of ultrapure water. The water pump was then activated at a speed of 86 μL min^{-1}. The eluted sample was collected every 5 minutes for the first 30 minutes and then every 15 minutes until reaching 8 hours. The Btz concentration in these samples was then analyzed with UV-vis spectroscopy. The best fitting was obtained with an S-curve $\left(\text{logistic function,} \left(\frac{a}{1 + be^{-kt}} + c\right)\right)$.

An Agilent Cary 60 UV-vis spectrophotometer in double beam mode was used for multiple experiments namely kinetic dissolution, soil leaching and photoprotection tests. The scans were collected in continuous mode between 600 nm and 200 nm in 1 mL quartz cuvettes. The calibration curve for quantitative assessment of bentazon was prepared and is presented in the ESI.†

Experiments on pea (phytotoxicity) and white mustard (efficacy) under controlled conditions

The phytotoxicity and efficacy of Btz-ACP nanoparticles as a nanoherbicide were tested on pea (Pisum sativum) as a standard rotation under the Mediterranean conditions, and white mustard (Sinapis alba) as a weed, respectively, under controlled conditions in growth chambers. The commercial variety of pea used for this study was Cartouche (LG Seeds, UK), while white mustard seeds were collected from the field in 2022. Seeds were pre-germinated to ensure the appropriate amount of plant material for the experiment procedure. A

This journal is © The Royal Society of Chemistry 2025

Environ. Sci.: Nano, 2025, 12, 4211–4221 | 4213

completely randomized block was designed with four plants per block (8 blocks × 32 repetitions × 4 treatments) in white mustard plants, and two plants per block (8 blocks × 16 repetitions × 4 treatments) in pea (Scheme S1†). Two pea and four white mustard germinated-seeds were sown in each 113 cm² plastic plant pot filled with a non-sterile 1 : 1 soil/sand mixture, and cultivated in a growth chamber at 22 ± 1 °C, illuminated with simulated sunlight (14 : 10 h light/dark cycle). The soil was collected from Cordoba, Southern Spain, which has a sandy loam soil type. Seedlings were sprayed with 20 mL of aqueous suspension (tap water) when the fourth leaf was completely unfolded. Plants were periodically irrigated with tap water. A commercial herbicide (Basagran®, 87% of Btz) was used as a positive control. Treatments and doses are presented in Table 1.

Phytotoxicity treatments. Four herbicide treatments were applied in pea plants: (i) Basagran® HD, (ii) Basagran® 2HD, (iii) Btz-ACP HD and (iv) Btz-ACP 2 HD, HD being the recommended dose for commercial bentazon 1.0 kg ha^{-1}. Different symptoms such as chlorosis or necrosis of leaf margins or in the entire leaves, and brown or yellow spots were observed. In addition to that, the plant height and number of new leaves were evaluated after 24 days post-treatment (dpt) to assess the phytotoxicity of the treatments.

Efficiency tests. White mustard plants were treated with four different herbicide treatments: (i) Basagran® HD; (ii) Basagran® 70% HD (0.7 kg ha^{-1} of Btz); (iii) Btz-ACP 60% HD (0.6 kg ha^{-1}); (iv) Btz-ACP 40% HD (0.4 kg ha^{-1}). The efficiency of the treatments was evaluated by mortality of plants at 10, 14 and 28 days. The percentage of mortality was evaluated using the following grade scale: 0–20%, plants slightly affected; 20–40%, 25% of plant tissue is affected; 50–60%, 50% of plant tissue is affected; 70–80%, plants seriously damaged showing 75% of tissue affected; 90%, almost dead plants with minimum photosynthetic area; 100%, dead plants. The evaluations were conducted by two independent evaluators.

Control plants either in phytotoxicity or efficiency experiments were set up as follows: untreated control group plants, receiving only tap water; treated control plants, receiving non-functionalized ACP nanoparticles at the same nanoparticle concentration (2HD for phytotoxicity tests and HD for efficiency experiments), and resuspended in tap water (Fig. S7 and S10†). Plants were evaluated ten and twenty-eight days after treatment as previously described.

Table 1 Summary of applied doses of the herbicide with reference to the active ingredient Btz quantity

Suggested higher dose Basagran®	1.15 kg ha^{-1}	
Treatment	kg Btz per ha	mg Btz per pot
HD	1.00	1.13
70% HD	0.70	0.79
60% HD	0.60	0.68
40% HD	0.40	0.45
2 HD	2.00	2.26

Nanoparticle aggregation at the applied dose

Dynamic light scattering (DLS) experiments were performed on Anton Paar Litesizer DLS 500 equipment, in backscatter orientation. The sample preparation involved diluting adsorbed nanoparticles at required concentrations mimicking three different concentrations, namely HD (reported as C1), 60% of HD (reported as C2) and an additional reduced dose of 40% of HD (reported as C3). All the samples were filtered with filter paper and subsequently with a nylon syringe filter with pores of 0.45 μm to remove the possible formation of very large aggregates. After this, the transmittance was in the range 80–90%, which is recommended to perform reliable DLS measurements. Non-filtered samples had a very low transmittance due to the high concentration (and aggregation), making the DLS measurement impossible. Hydrodynamic diameter distributions are shown as average of 10 repetitions.

Statistical analysis

The experimental design was developed as randomized blocks. Mortality data did not achieve normality and homogeneity requirements. Therefore, data were analyzed through a non-parametric Kruskal–Wallis test. Data processing and statistical analysis were carried out using SPSS software (version 25) (IBM Corp. released 2017, IBM SPSS Statistics for Windows, Version 25.0, Armonk, NY: IBM Corp).

Results and discussion

In this study, Btz-ACP was obtained through the functionalization of ACP nanoparticles (Fig. 1A). In the synthetic processes, the amorphous form was stabilized with citrate ions, since it has been found that citrate ions strongly interact with the Ca^{2+} ions of the apatite surface, inhibiting crystal thickening and stabilizing the size of the nanocrystals in bone.[43] Moreover, citrate plays an important role in stabilizing the transient amorphous phase, inhibiting the amorphous-to-crystalline conversion.[42,44] Subsequently, bentazon was adsorbed on the ACP nanoparticles with overnight stirring. It was then mixed with water for the overnight adsorption (see Materials and methods section for details). FTIR spectra show the typical poorly defined phosphate vibrational bands of amorphous calcium phosphate (Fig. 1B) along with citrate, carbonate and water bands, as previously reported for biomimetic ACP nanoparticles.[36] Moreover, the FTIR spectrum of Btz-ACP also displays the characteristic peaks of bentazon at around 1470 cm^{-1} (aromatic C=C bond region), 1340 cm^{-1} (CH bending of alkanes), 1250 cm^{-1} (S=O stretching) and 760 cm^{-1} (aromatic CH bending).[5] This finding indicated the successful functionalization of ACP with bentazon and can be compared with the control of ACP undergoing the same experimental conditions of adsorption, except for the addition of Btz (Fig. 1B, c). XRD patterns confirmed the
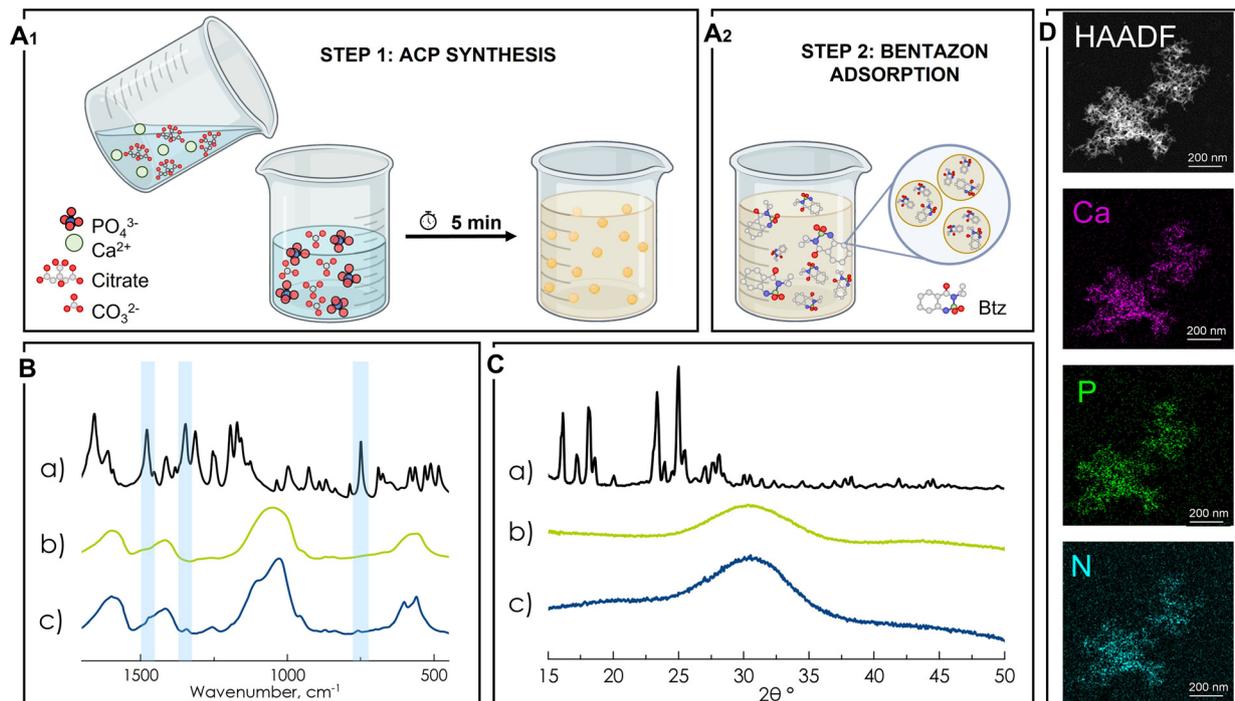
4214 | *Environ. Sci.: Nano*, 2025, **12**, 4211–4221

This journal is © The Royal Society of Chemistry 2025

Fig. 1 A) Synthetic procedure of ACP (A1) and Btz adsorption (A2). B) FTIR spectral comparison of a) commercial bentazon; b) ACP undergoing 24 hours of stirring in water : DMSO solution; c) Btz–ACP. All spectra were normalized. C) Powder X-ray diffraction patterns of a) commercial bentazon (ref. FAXVAB);[46] b) ACP undergoing 24 hours of stirring in water : DMSO solution; c) Btz–ACP. D) TEM micrographs with EDS elemental mapping of Btz-ACP nanocomposite. Elements are indicated on the image.

amorphous nature of Btz-ACP and the successful formation of a nanocomposite. In fact, the co-crystallization of the herbicide can be excluded by the absence of Bragg diffraction peaks associated with crystalline Btz (Fig. 1C, a and d). For instance, previous studies on the functionalization of nanocrystalline apatite with urea exhibited the undesired co-precipitation of crystalline urea (Bragg peaks associated with crystalline urea were clearly visible) rather than a pure urea-apatite nanocomposite, which would definitively compromise the benefits associated with nanosizing.[40,45]

The TEM micrograph of Btz-ACP (Fig. 1D and S4†) shows elongated nanoparticles resulting from the conversion of ACP into a more stable phase, poorly crystalline apatite during the functionalization, as previously observed during ACP functionalization with chemotherapeutic agents.[47,48] However, it is also important to remember that the XRD pattern of the bulk samples (Fig. 1C) did not exhibit Bragg peaks assignable to (nano-)crystalline phases, which indicate the lack of long-range crystalline order in the nanoparticles and confirm the amorphous nature of the nanoparticles. Studies of evolution of the crystalline phase at larger times are presented in the SI (Fig. S2†) and show the eventual conversion to the nanocrystalline phase after 50 days, without recrystallization of adsorbed Btz. The individual chemical maps obtained by EDS (Fig. 1D) exhibit a uniform distribution of nitrogen (blue), calcium (pink) and phosphorus (green), which indicate the homogeneous distribution of Btz on the calcium phosphate nanoparticles.

The elemental analysis revealed a loading of 4.5 ± 0.7 wt% of bentazon on Btz-ACP samples and the efficiency of the adsorption synthesis is 26.8%.

Release kinetics and leaching experiments of Btz-ACP

The release of bentazon in aqueous media was monitored by UV-vis for five days in a buffered solution at pH 7. As shown in Fig. 2A, Btz-ACP exhibited a gradual Btz release reaching the plateau within three days. The fitting of experimental data to a first order equation revealed a release rate constant for Btz-ACP of $k = 0.11$ h^{-1}. A comparison with the release in water of Btz can be made with the data of Azzali *et al.* already available in the literature,[5] showing that its dissolution is very fast and almost immediate with a constant rate of $k = 476$ h^{-1}. This controlled release mechanism holds the potential to prevent or minimize rain-induced wash-off of agrochemicals. Moreover, the solubility of the nanoparticles is pH-dependent, being stable at neutral pH but slightly soluble at acidic pH. To assess the pH-responsive release, Btz-ACP nanoparticles were tested at a pH of 4.5 in buffered solutions, revealing an increased release rate constant of $k = 0.20$ h^{-1} (Fig. S4†), which is more than two times higher than that in neutral Tris–HCl buffered solution. This would enable a slower or a faster delivery of the active ingredient in different plant tissues due to pH changes.[38,49] It has been demonstrated that calcium phosphate nanoparticles are able to penetrate the root and leaf epidermis, and subsequently

penetrate into deeper cell layers through the apoplast of epidermal and cortical cells, releasing their cargo inside the plant due to acidic conditions.[45,50,51]

Leaching experiments in a column filled with inert soil were conducted to compare the release kinetics of the commercial pesticide (Btz) and Btz-ACP (Fig. 2B). In these simulated soil column experiments, all the applied Btz leached through the 10 cm column. However, the retention difference was evident between the two formulations as the complete release occurred within 75 minutes for the conventional formulation, whereas in the nanoformulation Btz required 8 hours to pass through the column. Both processes follow first-order kinetics, but the rate constants differ by an order of magnitude, with $k = 0.1$ min^{-1} for Btz and $k = 0.01$ min^{-1} for Btz-ACP. Additionally, the leaching of the nanoformulation was clearly delayed compared to the free molecule, passing 90 min and 30 min, respectively, to elute the half of the added ingredients. This delay can be attributed to the slower release kinetics and the low water solubility of the nanoparticles; therefore the active ingredient

will be further retained in the soil. Reducing the mobility of the pesticide in soil is fundamental to reduce its leaching to other environments and groundwaters. Moreover, soil mobility of the pesticide influences microbial degradation along with other factors such as, soil pH, soil composition and application history.[52–54] The extension of pesticide residence time in the soil can enhance the efficacy of these microorganisms.[52] In fact, bentazon undergoes degradation in soil, facilitated by soil-dwelling bacteria and fungi at a moderate rate.[55] Nonetheless, a considerable amount of herbicide was found leaching through soil into groundwaters,[6,7,56] indicating that, due to the high mobility of bentazon, most of the applied active ingredients are not promptly degraded.

Evaluation of the herbicidal activity and phytotoxicity on model plants

The phytotoxicity of the commercial form of Btz (Basagran®) and Btz-ACP at the dose of Btz that is conventionally used (1 kg ha^{-1} as per product's commercial label) and double dose (2 kg ha^{-1}) was evaluated on pea (*Pisum sativum*) as a standard rotation under the Mediterranean conditions. Both Basagran® and Btz-ACP (Fig. S6† and 3A, respectively) did not induce toxicity effects on pea (*Pisum sativum*) even at double dose. The visual analysis of the treated pea plants demonstrated the absence of phytotoxic stress symptoms. The lack of visible signs of distress and mortality among the treated plants indicates that the nanoherbicide, at the applied doses, does not induce adverse effects on the physiology of pea plants and confirms its selectivity towards broadleaf weeds, minimizing the risk of non-target damage and ensuring the safety of the product's application. No significant growth promotion was observed either in plants treated with ACP or Btz-ACP, confirming the limited efficacy of unmodified nanosized calcium phosphate nanoparticles as a fertilizer in non-deficient plants.[57–59]

The efficacy of Btz-ACP and Basagran® at different doses was evaluated on white mustard (*Sinapis alba*) as the target plant. The results are presented in Fig. 3 and as can be seen in Fig. 3B, the plants were affected by a variety of symptoms and mortality in all the supplied treatments. In fact, compared with control plants, the symptoms that affected the plants were necrotic spots, large necrotic areas, and chlorotic areas of varying extent resulting in a reduction of the photosynthetic area of the plant (Fig. S8 and S9†).

Basagran® treatment at the highest dose of Btz (Fig. 3C, Basagran® 1.0 kg ha^{-1}) led to a mortality rate of 77.4 ± 24.5% after 10 days post-treatment (dpt), increasing to 91.7 ± 14.6% by 14 dpt, and then decreasing to 82.0 ± 28.1% by 28 dpt. Similar trends were observed with the reduced dose of Btz-ACP, where 60% of the active ingredient was applied (0.6 kg ha^{-1} Btz-ACP). In this scenario, mortality rates ranged from 78.1 ± 18.9% at 10 dpt to 91.0 ± 12.8% at 14 dpt, returning to 77.4 ± 29.7% at 28 dpt, showing no significant statistical difference compared to the higher dose of the commercial
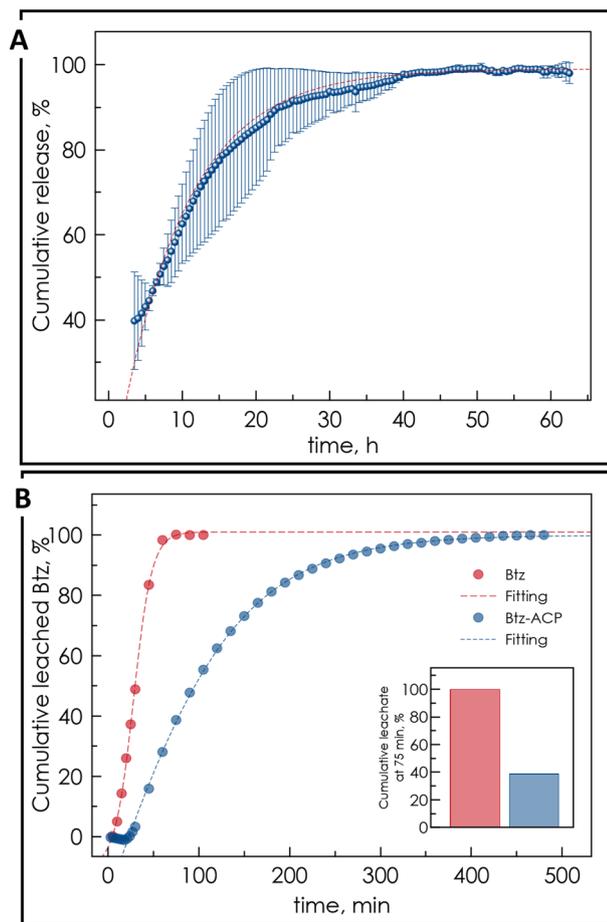
Fig. 2 A) Cumulative release of Btz from Btz-ACP in water. B) Leaching of the free molecule (Btz, red) and Btz-ACP (blue) in an inert soil medium during water irrigation. Differences between formulations at 75 minutes are shown in the inset. Experimental data (dots) are expressed as mean. The dashed line represents the best fits of the experimental data.

4216 | *Environ. Sci.: Nano*, 2025, **12**, 4211–4221
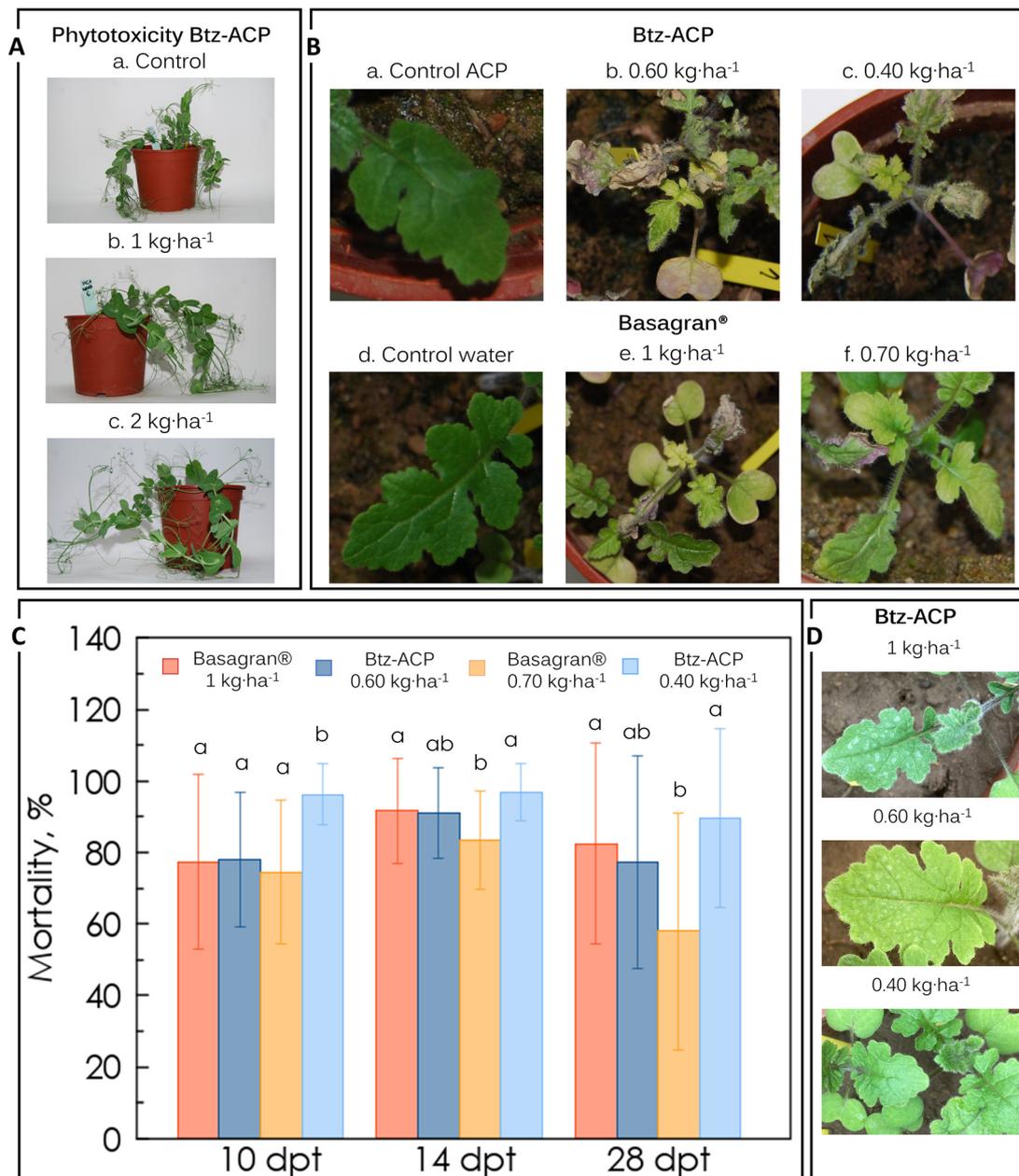
This journal is © The Royal Society of Chemistry 2025

Fig. 3 A) Phytotoxicity experiments on *Pisum sativum* plants, treated with Btz-ACP, 24 days after treatment. B) Evaluation of the efficiency 28 days after treatment application. Representative pictures of the symptoms on *Sinapis alba*: above treatment with Btz-ACP ((a) control ACP, (b) 0.60 kg ha⁻¹, and (c) 0.4 kg ha⁻¹); and Basagran® as the commercial Btz treatment ((d) control water, (e) 1 kg ha⁻¹, and (f) 0.70 kg ha⁻¹). C) Graphical representation of incidence of mortality in *Sinapis alba* plants. Values of mortality (%) at 10, 14 and 28 days post treatment. In blue and light blue, Btz-ACP treatments at 0.60 kg ha⁻¹ and 0.4 kg ha⁻¹, and in red and orange, Basagran treatments at 1 kg ha⁻¹ and 0.70 kg ha⁻¹. Data are averaged (*n* = 32), error bars represent standard deviation, data with the same letter are not significantly different, different treatments within the same day were compared (Kruskal–Wallis test, $p < 0.05$). D) Images of leaf retention of Btz-ACP at three different dilutions of the nanoformulation to assess visually leaf retention of the nanoparticles and effects of increasing dilutions.

compound (Basagran® at 1.0 kg ha⁻¹). However, when compared with the reduced dose of Basagran®, where 70% of the active ingredient was applied (0.7 kg ha⁻¹), the formulation exhibited inefficient weed control. Mortality rates ranged from 74.5 ± 20.1% to 83.4 ± 13.7% at 10 and 14 dpt, respectively, but dropped significantly to 57.9 ± 33.2% at 28 dpt. These findings indicate that the nanoherbicide allows

the reduction of the bentazon dose from 1.0 kg ha⁻¹ to 0.6 kg ha⁻¹, without compromising the herbicidal activity.

Surprisingly, the higher reduction of the dosage with the nanoparticles (Btz-ACP 0.4 kg ha⁻¹) showed enhanced herbicide activity. In fact, already at 10 dpt, increased mortality rates were observed at 96.3 ± 8.8%, showing statistically significant differences with respect to all other

This journal is © The Royal Society of Chemistry 2025

Environ. Sci.: Nano, 2025, **12**, 4211–4221 | **4217**

treatments ($p < 0.05$, Fig. 3C). Moreover, this mortality rate increased after 14 dpt ($96.9 \pm 8.1\%$) and remained constant (89.7 ± 25.1) after 28 dpt, both statistically different from Basagran® at 0.7 kg ha^{-1}. This indicates that Btz-ACP at a reduced dosage of 0.4 kg ha^{-1} is more effective and acts faster than its higher dose counterparts, providing prolonged herbicidal activity. These interesting results indicate that the dose of bentazon could be reduced by up to 60% compared to the recommended commercial formulations.

The sustained efficacy of the nanoherbicide may be attributed to multifactorial and complex mechanisms, stemming from the unique characteristics of the nanoparticles and the specific treatment method employed. Primarily, the treatments were administered *via* foliar spray application, which is the recommended method for Basagran application. This can be advantageous for the nanoformulation in general, as previous studies have demonstrated that nanoparticles can specifically interact with leaf surfaces, allowing them to remain attached to the leaf surface (see Fig. 3D).[38,39] This can help reduce both leaching and treatment wash off, thereby enhancing its efficiency and retaining the active ingredient on the plant. Additionally, the delayed release of the active molecule, as indicated by our data (Fig. 2A), can facilitate the prolonged supply of Btz to the plant over an extended period. Moreover, the nanosized nature of the treatment suggests better treatment–plant interaction and efficacy, as previously demonstrated by multiple studies.[60,61] Understanding the precise interactions between nanoparticles and plant tissues is challenging. However, the reduced size of the nanoparticles likely enhances plant uptake through stomata and cuticles. This facilitates the entry of ACP into the plant and the subsequent gradual release of the active molecule.[62–64]

Regarding this point, an interesting result of this research is the different efficacy of the nano-based treatments that suggests better performances at highly reduced doses (0.4 kg ha^{-1}). The counterintuitive behavior observed with the two doses of nanoherbicide can be attributed to multiple factors. These may include the intrinsic properties of the new material, its interactions with the organism, and/or the treatment conditions. Notably, the authors suggest that these effects may be related to the aggregation dynamics of the different nanosystems. Specifically, nanoparticles at lower concentrations exhibit reduced aggregation, resulting in a more homogeneous distribution on the plant surfaces. Furthermore, as observed in the images in Fig. 3D, white spots are present in greater quantities at higher doses of the treatment but not visible in the more diluted ones, the penetration of the nanoparticles being favored at lower concentrations (lower aggregation).

To confirm this hypothesis, we studied the size (hydrodynamic diameter) distributions of Btz-ACP at various concentrations simulating the different treatments. Dynamic light scattering (DLS) analysis confirmed the formation of large aggregates, with hydrodynamic diameters of 611 ± 109
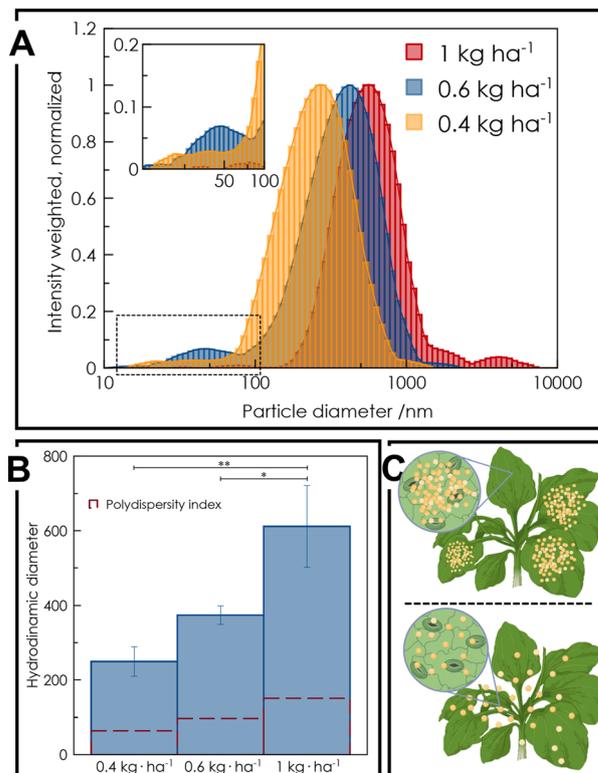

Fig. 4 Study of the aggregation of different dilutions of Btz-ACP simulating 1 kg ha^{-1}, 0.6 kg ha^{-1}, and 0.4 kg ha^{-1}. A) Intensity-weighted size (hydrodinamic diameter) distributions. The inset in A) represents a zoom-in of the size distribution as indicated. B) DLS analysis shows that the hydrodynamic diameter (Z-average) increases with the concentration. C) Graphical scheme representing the concentration-dependent particle aggregation with the corresponding accumulation of large aggregates on the leaves at high concentrations (top), not observed at lower concentrations (bottom), where the penetration is thus favored, resulting in a longer effect of the herbicide. Statistical analysis in (B) was performed using the one-way ANOVA test and Bonferroni's *post hoc* test. *p-value < 0.05, **p-value < 0.01.

nm for the highest concentration (C1, simulating 1 kg ha^{-1}), 373 ± 25 nm for the intermediate concentration (C2, simulating 0.6 kg ha^{-1}), and 249 ± 40 nm for the most diluted sample (C3, simulating 0.4 kg ha^{-1}). Hydrodynamic diameters with polydispersity index are depicted in Fig. 4 and intensity-weighted particle distribution peaks are shown that exhibit similar patterns across different concentrations, with some overlap between peaks.

These differences in nanoparticle dimensions are due to the aggregating tendency of the system that is more pronounced at higher concentrations. Remarkably, all the measurements were performed after filtering the samples (pore size = 0.45 μm), since without filtering small nanoparticles remained concealed beneath the larger ones, rendering their detection challenging (see further details in Materials and methods). Overall, these very large (micrometric) particles are less apt to significantly contribute to the efficacy of the nanoherbicide, given their hindered penetration into plant tissues due to their size. Conversely, smaller nanoparticles, whose diameter and

4218 | *Environ. Sci.: Nano*, 2025, **12**, 4211–4221

This journal is © The Royal Society of Chemistry 2025

numbers decrease with decreasing concentration, are anticipated to play a pivotal role in the action of the nanoherbicides. In this type of system this has rarely been investigated; therefore this is a very interesting breakthrough for future research.

More precisely, it appears that the nanosizing of the herbicide contributes more to the efficiency of the treatment when the nanoparticles are more diluted, that is less aggregated, but the contribution of the burst released bentazon is more pronounced when the nanosizing is not as effective because of aggregation at higher concentrations. It must be noted that roughly 40% of the adsorbed active ingredient is probably physiosorbed to the nanoparticles, as evidenced by the release kinetics in water (Fig. 2A), and that is probably the one acting first and most at higher concentrations.

Conclusions

In conclusion, a post-emergence herbicide was loaded on the surface of biocompatible and biodegradable calcium phosphate nanoparticles. The characteristics and performances of the resulting nanocomposite were studied in detail. FTIR spectroscopy and elemental analysis confirmed the successful loading of bentazon on the nanoparticles (4.5 ± 0.7 wt%). In addition, structural analysis confirmed that Btz did not recrystallize during the synthetic process, but was instead adsorbed on the nanoparticles, confirming the successful production of an organic/inorganic nanocomposite. Furthermore, the release of the active ingredient from the nanoparticles in aqueous media and soil demonstrated a slower release rate compared to the formulation as sodium salts. This observation is noteworthy, especially in soil release, as it suggests the potential for increased degradation by soil bacteria and this feature holds significance in the context of reduced pollution of soils and groundwaters.

In vivo plant experiments proved the efficacy and higher efficiency of the new nanoherbicide in weed control, as it demonstrated to be acting faster and more efficiently than its commercial counterparts. Reduced doses of nanoparticles proved to be selectively killing the target plant and additionally controlling the regrowth of plants over long periods, while allowing for an overall reduction of at least 60% of the active ingredient to attain the same results. Variances between applications at different doses were evaluated and justified with increased aggregation of the nanoparticles at higher concentrations. This is indeed a relevant insight for future studies related to the application of nanomaterials for the efficient delivery of active species (nutrients, biostimulants, pesticides, *etc.*) in plants. Overall, all these results contribute to the proposal of this material as a promising new formulation for the delivery of the herbicide bentazon with multiple advantages owing to its nanosize, that is at times based on the biocompatible and biodegradable green synthesized material and it provides more efficient weed control.

Data availability

The data supporting this article have been included as part of the ESI.† We are willing to share research data with interested researchers. Data are available to all upon request; please contact the authors of this manuscript.

Author contributions

A. A. experiments on the material and C. M. R. *in vivo* plant experiments, with the technical support of M. C. A. B.; A. A., C. M. R., B. P. T. and G. B. R. R. investigation, formal analysis and data curation; A. A. and J. M. D. L. conceptualization of the project and wrote the first version of the manuscript with support from B. P. T. and G. B. R. R.; A. A., A. P. L., F. G. and J. M. D. L. funding and revisions; J. M. D. L. and A. P. D. L. supervision.

Conflicts of interest

There are no conflicts to declare. The authors would like to inform that a patent (P202530383) has been filed with part of the results reported on this manuscript.

References

1 *A Farm to Fork Strategy for a fair, healthy and environmentally-friendly food system*, 2020.

2 A. Sharma, V. Kumar, B. Shahzad, M. Tanveer, G. P. S. Sidhu, N. Handa, S. K. Kohli, P. Yadav, A. S. Bali, R. D. Parihar, O. I. Dar, K. Singh, S. Jasrotia, P. Bakshi, M. Ramakrishnan, S. Kumar, R. Bhardwaj and A. K. Thukral, *SN Appl. Sci.*, 2019, **1**, 1446.

3 J. M. M. Oliveira, V. Galhano, I. Henriques, A. M. V. M. Soares and S. Loureiro, *Environ. Pollut.*, 2017, **221**, 52–63.

4 K. N. Reddy, M. A. Locke and K. D. Howard, *Weed Technol.*, 1995, **9**, 773–778.

5 A. Azzali, S. d'Agostino and F. Grepioni, *ACS Sustainable Chem. Eng.*, 2021, **9**, 12530–12539.

6 F. A. Swartjes and M. Van der Aa, *Sci. Total Environ.*, 2020, **699**, 134186.

This journal is © The Royal Society of Chemistry 2025

Environ. Sci.: Nano, 2025, **12**, 4211–4221 | **4219**

7 S. Giuliano, L. Alletto, C. Deswarte, F. Perdrieux, J. Daydé and P. Debaeke, *Sci. Total Environ.*, 2021, **788**, 147695–147695.

8 M. V. Barbieri, A. Peris, C. Postigo, A. Moya-Garcés, L. S. Monllor-Alcaraz, M. Rambla-Alegre, E. Eljarrat and M. López de Alda, *Environ. Pollut.*, 2021, **274**, 115813.

9 M. J. Carrizosa, M. J. Calderón, M. C. Hermosín and J. Cornejo, *Sci. Total Environ.*, 2000, **247**, 285–293.

10 H. F. H. Abouziena, S. D. Sharma and M. Singh, *Crop Prot.*, 2009, **28**, 1081–1085.

11 M. A. Balah, A. Hanafi and S. B. A. Ghani, *J. Environ. Sci. Health, Part B*, 2012, **47**, 390–396.

12 A. Nayak, P. Chaudhary, B. Bhushan, K. Ghai, S. Singh and M. Sillanpää, *Int. J. Biol. Macromol.*, 2024, **258**, 129092.

13 B. C. D. S. Rocha, L. E. Z. D. Moraes, D. E. Santo, A. P. Peron, D. C. D. Souza, E. Bona and O. Valarini, *J. Chem. Technol. Biotechnol.*, 2024, **99**, 1342–1355.

14 L. Wang, J. Wang, Y. Wang, Y. Qin and Y. Zhou, *J. Mol. Liq.*, 2023, **387**, 122705.

15 A. Spaltro, S. Simonetti, S. Laurella, D. Ruiz, A. D. Compañy, A. Juan and P. Allegretti, *J. Contam. Hydrol.*, 2019, **227**, 103542.

16 A. B. Ribeiro, E. P. Mateus and J.-M. Rodríguez-Maroto, *Sep. Purif. Technol.*, 2011, **79**, 193–203.

17 S. Saranya, R. Aswani, A. Remakanthan and E. K. Radhakrishnan, in *Nanotechnology for Agriculture: Advances for Sustainable Agriculture*, ed. D. G. Panpatte and Y. K. Jhala, Springer, Singapore, 2019, pp. 1–17.

18 D. Wang, N. B. Saleh, A. Byro, R. Zepp, E. Sahle-Demessie, T. P. Luxton, K. T. Ho, R. M. Burgess, M. Flury, J. C. White and C. Su, *Nat. Nanotechnol.*, 2022, **17**, 347–360.

19 M. Kah, R. S. Kookana, A. Gogos and T. D. Bucheli, *Nat. Nanotechnol.*, 2018, **13**, 677–684.

20 Z. Xu, T. Tang, Q. Lin, J. Yu, C. Zhang, X. Zhao, M. Kah and L. Li, *Environ. Chem. Lett.*, 2022, **20**, 2097–2108.

21 M. M. L. Forini, M. S. Pontes, D. R. Antunes, P. H. C. D. Lima, J. S. Santos, E. F. Santiago and R. Grillo, *Plant Nano Biol.*, 2022, **1**, 100008.

22 K. Kusumavathi, S. K. Rautaray, S. Sarkar, S. Dash, T. R. Sahoo, S. K. Swain and D. Sethi, *Plant Nano Biol.*, 2025, **11**, 100132.

23 V. Takeshita, F. F. Oliveira, A. Garcia, N. Zuverza-Mena, C. Tamez, B. C. Cardoso, C. W. Pinácio, B. Steven, J. LaReau, C. E. Astete, C. M. Sabliov, L. F. Fraceto, V. L. Tornisielo, C. O. Dimkpa and J. C. White, *Environ. Sci.: Nano*, 2025, **12**, 388–404.

24 V. Takeshita, A. C. Preisler, G. V. Munhoz-Garcia, L. B. Carvalho, C. de W. Pinácio, H. C. Oliveira, V. L. Tornisielo, B. C. Cardoso, E. F. B. Ramalho, R. F. Pimpinato, A. M. Dionisio, W. A. Verri and L. F. Fraceto, *Environ. Sci.: Nano*, 2024, **11**, 4536–4550.

25 B. T. Sousa, L. B. Carvalho, A. C. Preisler, T. Saraiva-Santos, J. L. Oliveira, W. A. Verri Jr., G. Dalazen, L. F. Fraceto and H. Oliveira, *ACS Appl. Mater. Interfaces*, 2025, **17**, 13122–13134.

26 J. Dong, X. Liu, Y. Chen, W. Yang and X. Du, *J. Colloid Interface Sci.*, 2021, **594**, 20–34.

27 J. Dong, G. Wang and X. Li, *et al.*, *J. Adv. Res.*, 2024, DOI: 10.1016/j.jare.2024.12.005.

28 H. Wang, G. Tang, Z. Zhou, X. Chen, Y. Liu, G. Yan, X. Zhang, X. Li, Y. Huang, J. Wang and Y. Cao, *ACS Appl. Mater. Interfaces*, 2023, **15**, 4303–4314.

29 V. Takeshita, L. B. Carvalho, J. A. Galhardi, G. V. Munhoz-Garcia, R. F. Pimpinato, H. C. Oliveira, V. L. Tornisielo and L. F. Fraceto, *ACS Nanosci. Au*, 2022, **2**, 307–323.

30 L. B. Carvalho, I. S. Godoy, A. C. Preisler, P. L. de F. Proença, T. Saraiva-Santos, W. A. Verri, H. C. Oliveira, G. Dalazen and L. F. Fraceto, *Environ. Sci.: Nano*, 2023, **10**, 1629–1643.

31 R. Boukhalfa, C. O. Dimkpa, C. Deng, Y. Wang, C. Ruta, G. J. Calabrese, S. Messgo-Moumene, A. Bharadwaj, R. Muthuramalingam, J. C. White and G. De Mastro, *ACS Agric. Sci. Technol.*, 2024, **4**, 1321–1331.

32 Y. Zeng, X. Li, F. Chen, H. Ye, K. Rong, Z. Ran, B. Liu, Z. Pan, X. Xie, J. Tang, X. Liu and Y. He, *J. Environ. Chem. Eng.*, 2024, **12**, 112572.

33 Y. Xiang, J. Han, G. Zhang, F. Zhan, D. Cai and Z. Wu, *ACS Sustainable Chem. Eng.*, 2018, **6**, 3649–3658.

34 A. Mech, S. Gottardo, V. Amenta, A. Amodio, S. Belz, S. Bøwadt, J. Drbohlavová, L. Farcal, P. Jantunen, A. Małyska, K. Rasmussen, J. Riego Sintes and H. Rauscher, *Regul. Toxicol. Pharmacol.*, 2022, **128**, 105093.

35 M. Epple, *Acta Biomater.*, 2018, **77**, 1–14.

36 G. B. Ramírez-Rodríguez, G. Dal Sasso, F. J. Carmona, C. Miguel-Rojas, A. Pérez-de-Luque, N. Masciocchi, A. Guagliardi and J. M. Delgado-López, *ACS Appl. Bio Mater.*, 2020, **3**, 1344–1353.

37 Y. Sakhno, L. Degli Esposti, A. Adamiano, J. Borgatta, M. Cahill, S. Vaidya, J. C. White, M. Iafisco and D. P. Jaisi, *ACS Agric. Sci. Technol.*, 2023, **3**, 845–854.

38 B. Parra-Torrejón, A. Cáceres, M. Sánchez, L. Sainz, M. Guzmán, F. J. Bermúdez-Perez, G. B. Ramírez-Rodríguez and J. M. Delgado-López, *Environ. Sci. Technol.*, 2023, **57**, 14950–14960.

39 B. Parra-Torrejón, G. B. Ramírez-Rodríguez, M. J. Giménez-Bañón, J. D. Moreno-Olivares, D. F. Paladines-Quezada, R. Gil-Muñoz and J. M. Delgado-López, *Environ. Sci.: Nano*, 2021, **8**, 3524–3535.

40 N. Kottegoda, C. Sandaruwan, G. Priyadarshana, A. Siriwardhana, U. A. Rathnayake, D. M. Berugoda Arachchige, A. R. Kumarasinghe, D. Dahanayake, V. Karunaratne and G. A. J. Amaratunga, *ACS Nano*, 2017, **11**, 1214–1221.

41 J. M. Delgado-López, R. Frison, A. Cervellino, J. Gómez-Morales, A. Guagliardi and N. Masciocchi, *Adv. Funct. Mater.*, 2014, **24**, 1090–1099.

42 J. M. Delgado-López, M. Iafisco, I. Rodríguez, A. Tampieri, M. Prat and J. Gómez-Morales, *Acta Biomater.*, 2012, **8**, 3491–3499.

43 Y.-Y. Hu, A. Rawal and K. Schmidt-Rohr, *Proc. Natl. Acad. Sci. U. S. A.*, 2010, **107**, 22425–22429.

4220 | *Environ. Sci.: Nano*, 2025, **12**, 4211–4221

This journal is © The Royal Society of Chemistry 2025

44 Y. Chen, W. Gu, H. Pan, S. Jiang and R. Tang, *CrystEngComm*, 2014, **16**, 1864–1867.

45 B. Sharma, H. Kohay, S. Sharma, M. Youngblood, J. P. Cochran, J. M. Unrine, O. V. Tsyusko, G. V. Lowry and J. P. Giraldo, *ACS Nano*, 2025, **19**, 3906–3919.

46 L. E. Moss, B. A. Karcher, J. W. Richardson and R. A. Jacobson, *Acta Crystallogr., Sect. C: Cryst. Struct. Commun.*, 1986, **42**, 1785–1787.

47 C. Mesas, V. Garcés, R. Martínez, R. Ortiz, K. Doello, J. M. Dominguez-Vera, F. Bermúdez, J. M. Porres, M. López-Jurado, C. Melguizo, J. M. Delgado-López and J. Prados, *Biomed. Pharmacother.*, 2022, **155**, 113723.

48 F. Quiñonero, B. Parra-Torrejón, G. B. Ramírez-Rodríguez, V. Garcés, J. M. Delgado-López, C. Jiménez-Luna, G. Perazzoli, C. Melguizo, J. Prados and R. Ortíz, *Int. J. Nanomed.*, 2023, **18**, 5075–5093.

49 I. Rodríguez-Ruiz, J. M. Delgado-López, M. A. Durán-Olivencia, M. Iafisco, A. Tampieri, D. Colangelo, M. Prat and J. Gómez-Morales, *Langmuir*, 2013, **29**, 8213–8221.

50 A. E. Szameitat, A. Sharma, F. Minutello, A. Pinna, M. Er-Rafik, T. H. Hansen, D. P. Persson, B. Andersen and S. Husted, *Environ. Sci.: Nano*, 2021, **8**, 444–459.

51 G. B. Ramírez-Rodríguez, C. Miguel-Rojas, G. S. Montanha, F. J. Carmona, G. Dal Sasso, J. C. Sillero, J. Skov Pedersen, N. Masciocchi, A. Guagliardi, A. Pérez-de-Luque and J. M. Delgado-López, *Nanomaterials*, 2020, **10**, 1043.

52 M. Arias-Estévez, E. López-Periago, E. Martínez-Carballo, J. Simal-Gándara, J.-C. Mejuto and L. García-Río, *Agric., Ecosyst. Environ.*, 2008, **123**, 247–260.

53 S. C. Wagner, R. M. Zablotowicz, L. A. Gaston, M. A. Locke and J. Kinsella, *J. Agric. Food Chem.*, 1996, **44**, 1593–1598.

54 A. Boivin, R. Cherrier, C. Perrin-Ganier and M. Schiavon, *Pest Manage. Sci.*, 2004, **60**, 809–814.

55 J. da Silva Coelho, C. G. M. de Souza, A. L. de Oliveira, A. Bracht, M. A. F. Costa and R. M. Peralta, *Curr. Microbiol.*, 2010, **60**, 350–355.

56 A. Schuhmann, G. Klammler, S. Weiss, O. Gans, J. Fank, G. Haberhauer and M. H. Gerzabek, *Plant, Soil Environ.*, 2019, **65**, 273–281.

57 D. Montalvo, M. J. McLaughlin and F. Degryse, *Soil Sci. Soc. Am. J.*, 2015, **79**, 551–558.

58 R. Liu and R. Lal, *Sci. Rep.*, 2014, **4**, 5686.

59 L. Xiong, P. Wang, M. N. Hunter and P. M. Kopittke, *Environ. Sci.: Nano*, 2018, **5**, 2888–2898.

60 S. Kumar, M. Nehra, N. Dilbaghi, G. Marrazza, A. A. Hassan and K.-H. Kim, *J. Controlled Release*, 2019, **294**, 131–153.

61 R. Nair, S. H. Varghese, B. G. Nair, T. Maekawa, Y. Yoshida and D. S. Kumar, *Plant Sci.*, 2010, **179**, 154–163.

62 V. Takeshita, B. T. de Sousa, A. C. Preisler, L. B. Carvalho, A. do E. S. Pereira, V. L. Tornisielo, G. Dalazen, H. C. Oliveira and L. F. Fraceto, *J. Hazard. Mater.*, 2021, **418**, 126350–126350.

63 A. Avellan, J. Yun, Y. Zhang, E. Spielman-Sun, J. M. Unrine, J. Thieme, J. Li, E. Lombi, G. Bland and G. V. Lowry, *ACS Nano*, 2019, **13**, 5291–5305.

64 T. Eichert, A. Kurtz, U. Steiner and H. E. Goldbach, *Physiol. Plant.*, 2008, **134**, 151–160.

This journal is © The Royal Society of Chemistry 2025

Environ. Sci.: Nano, 2025, **12**, 4211–4221 | **4221**